Effects of Layer-Charge Distribution on Swelling Behavior of Mixed-Layer Illite-Montmorillonite Clays: A Molecular Dynamics Simulation Study

Article *in* Journal of Molecular Liquids · April 2021

DOI: 10.1016/j.molliq.2021.116188

2 authors, including:

Me Ghasemi
Nazarbayev University
6 PUBLICATIONS **27** CITATIONS

SEE PROFILE

Journal of Molecular Liquids 335 (2021) 116188

Contents lists available at ScienceDirect

Journal of Molecular Liquids

journal homepage: www.elsevier.com/locate/molliq

Effects of layer-charge distribution on swelling behavior of mixed-layer illite-montmorillonite clays: A molecular dynamics simulation study

Mehdi Ghasemi, Mohammad Sharifi *

Department of Petroleum Engineering, Amirkabir University of Technology, Tehran, Iran

ARTICLE INFO

Article history:
Received 30 March 2021
Accepted 13 April 2021
Available online 17 April 2021

Keywords:
Mixed-layer illite-montmorillonite clays
Swelling
Charge distribution
Molecular dynamics simulation

ABSTRACT

One of the intriguing properties of clay minerals is swelling, which is considered an essential characteristic for various geological processes, environmental science, and engineering. Almost all previous experimental and simulation studies focused on the understanding of the swelling behavior of pure clays. The fact is that about 30 percent of all clays are a pure type, and virtually 70 percent of clays are the mixed-layer one that swelling mechanism is still elusive. In this research, molecular dynamics simulations were used to exclusively investigate the effect of layer charge distribution on the crystalline swelling and hydration behavior of the most common types of mixed clays, so-called illite-montmorillonite mixed-layer clay (I-Mt MLC) with Na^+ and K^+ counterions in the presence of different water concentrations. Based on the results, we found that the layer charge density and charge location of both illite and Mt significantly influenced the I-Mt clays' swelling behavior. Regardless of Mt charge density, the presence of highly charged illite led to powerful interactions of counterions with the surface sheet, resulting in less swelling behavior of the I-Mt system. Also, the various polarization power of clay surface due to the difference in charge distribution of octahedral sheets had a significant influence on water molecules and interlayer cations interaction with clay surface, which affected the swelling behavior of I-Mt clays. Overall, our findings demonstrated the new insight into I-Mt clays' swelling behavior, which is a function of charge distribution of both illite and Mt.

1. Introduction

Clay minerals, as fine-grained and porous materials, are formed in the weathering and pedogenic processes and constitute a large portion of soils and sediments [1]. Clays are characterized by a large surface area, strong adsorption capacity, and high swelling capacity, which make them valuable compounds in a broad spectrum of applications of environmental remediation [2,3] geological processes [4-6], nuclear waste disposal [7-10] chemical catalysis [11-13], drug delivery [14-16], and in drilling fluids to modify the rheology and control the borehole stability of oil and gas wells [17-20]. In particular, the swelling behavior of clays is of significant importance in the oil and gas industry, as clays in various types are found in geological formation as well as drilling fluids. In fact, during the drilling operation, water interactions as a base of major drilling fluids with clayey formations can cause swelling, which results in wellbore instability. Therefore, understanding the swelling behavior of clayey formation is a critical factor in the successful design of drilling fluid and utilizing the proper clay swelling inhibitors [19,21].

According to the previous studies, the swelling behavior of clays exhibits two stepwise regimes, including crystalline and osmotic swelling [22,23]. Crystalline swelling of clay minerals occurs in a stepwise formation of one to three hydration states from the dehydrated state through a gradual increase of water adsorption in the clay interlayer. The interlayer space ranges from 9 to around 19 Å for crystalline swelling [24-26]. Virtually all types of clay minerals display crystalline swelling in the presence of a water solution. Osmotic swelling occurs due to an increase in interlayer water intake from an aqueous solution that culminates in interlayer expansion from 20 to 130 Å [25,27,28]. Contrary to crystalline swelling, osmotic swelling of clay minerals is only limited to some specific clays [29,30].

There are comprehensive studies of interlayer swelling on pure clay systems. Based on previous researches, various influencing factors have been introduced to understand the swelling behaviors of clay minerals. Factors related to the clay such as charge site location and charge density [26,27,29-31], ion size [22,32,33], ion charge [32-34], and identity of interlayer ions [24,29,35,36] can affect clay swelling. As stated previously, the swelling properties

* Corresponding author.
E-mail address: m_sharifi@aut.ac.ir (M. Sharifi).

https://doi.org/10.1016/j.molliq.2021.116188
0167-7322/

of clay minerals are not the same in which Na^+-montmorillonite (Na^+-Mt) tends to swell easily from monolayer hydration state up to osmotic swelling, while K^+-illite (K^+-I) has less tendency to swell [36]. Regarding the impact of charge location and charge density on clay swelling, previously reported results are restricted, and drawing the exact conclusions is nearly impossible. For example, Liu and Lu [36] showed that in large charge density on tetrahedral sheets, clay interlayer experiences more expansion compared to clay with a high charge density of octahedral sheets. These comparisons were conducted for three different water contents. In comparing the swelling behavior of Otay- montmorillonite (Otay-Mt), in which concentration of charge is on octahedral sheets with Wyoming-Mt that has less charge density on octahedral sheets, Chávez-Páez et al. [38] revealed that interlayer expansion of the Otay-Mt is lower than Wyoming-Mt. Smith et al. [39] assessed the effect of octahedral charge density on swelling of Na-Mt, and they found that more charge density on octahedral sheets results in higher interlayer expansion. However, Foster [40] reported a reduction in swelling of Mt as the charge density of octahedral sheets increases. Seppälä et al. [41] claimed that the smaller the layer charge, the greater swelling would result. Sun [42] and Greathouse et al. [43] found similar results. Skipper et al. [44] reported that increasing the tetrahedral charge layer of Na^+-Mt leads to increasing interlayer expansion. Interaction of water with Mt and beidellite was studied by Teich-McGoldrick et al. [29]. They showed that in the case of low water content between interlayers, beidellite, which has a similar structure to illite, expands more than Mt. However, Mt showed more interlayer expansion at a high water content. Also, they observed that the beidellite formed the bilayer hydration state at low water content compared to Mt. More recently, Li et al. [37] found that clay minerals with different charge locations and charge densities display divergent swelling behaviors. They showed that K^+ has dual characteristics in which their behavior as swelling inhibitors relies on the charge location of clay. However, Ferrage et al. [45] reported that due to the low hydration of K^+ and their perturbable characteristics, they could act as a clay swelling inhibitor.

Most of the studies related to clay swelling have been focused on pure clays. In 2018, for the first time, the swelling behavior of mixed-layer clays (MLCs), including I-Mt clays for a wide range of water concentrations in the presence of Na^+ and K^+, were investigated [46]. They showed that the swelling behavior of I-Mt is significantly different from pure clay and depends on both clay types and interlayer cations. More recently, a comprehensive study was conducted on the swelling behavior of a chlorite-montmorillonite mixed-layer clay (CH-Mt MLC) as a function of interlayer cation including Na^+, K^+, and Cs^+ [47].

The fact is that in addition to the pure clays, plenty of MLCs can be found in various types of sedimentary rocks [48,49]. Among different kinds of MLCs, illite-montmorillonite (I-Mt) is the most abundant compared to others such as CH-Mt or even illite-chlorite-montmorillonite (I-CH-Mt). As previously mentioned, various factors affect the swelling behavior of pure clays. However, these factors may have different influences on the swelling behavior of MLCs. In the present study, we focused on I-Mt MLCs. As is known, both the illite and Mt consist of negatively charged octahedral sheets of alumina (O) and tetrahedral sheets of silica (T). They are categorized as TOT type clay which means that the octahedral sheet is located between two tetrahedral sheets. The negative charge of layers comes from the isomorphic substitution of layers in which Si^{+4} is replaced with Al^{+3} in tetrahedral sheets, and Al^{3+} in octahedral sheets is substituted with Mg^{2+}. The major difference between the two mentioned clays is related to the location of isomorphic substitution. Most of the charge distribution of illite and Mt are on the tetrahedral and octahedral sheets, respectively. The interlayer counterions of Mt can be Na^+, Ca^{2+}, and Mg^{2+}, and the negative charge of illite is balanced by K^+. As previously mentioned, the nature of these cations also greatly influences the swelling of clays. Therefore, the presence of two types of counterions, in this study Na^+ and K^+, with various concentrations between the two different clay sheets makes swelling process analysis more complex.

Almost all previous investigations of the effects of charge distribution on clay swelling behavior have been limited to pure clay to date except works by Rahromostaqim and Sahimi [46,47]. However, no comprehensive research has been conducted on the I-Mt MLCs with various charge densities and charge locations to know their effects on swelling behavior. In this work, the impacts of the surface charge distribution by considering charge density and charge location on the swelling behavior of K^+-illite-Na^+-montmorillonite (K^+-I-Na^+-Mt) were investigated for a wide range of water concentrations. Four mixed layers I-Mt clay mineral structures with different charge densities (i.e., high charge (HC) and low charge (LC)) were considered. The molecular dynamics (MD) simulation technique has been applied to provide insight into the effects of the mentioned factors. To better understand the swelling mechanism, the results obtained from swelling behavior analyses of the pure Mt and pure illite interlayers are regarded as a reference for comparison with the other simulated cases.

The remainder of this paper is organized as follows. First, we describe the simulation systems and procedures in Section 2. Then, the results are presented in Section 3, and the summary of the paper is drawn in the last section.

2. Methodology

2.1. Model construction

The 2:1 clay mineral models were constructed based on the pyrophyllite structure with a chemical formula of $Al_4Si_8O_{20}(OH)_4$. The lattice parameters of the pyrophyllite unit cell are: a = 5.16 Å, b = 8.97 Å, and c = 9.37 Å, and $\alpha = 91.5°$, $\beta = 100.46°$, and $\gamma = 89.6°$ [50]. As is mentioned, Na^+-Mt and K^+-I were used with different charge site locations and charge densities on the octahedral and tetrahedral sheets to assess the swelling behavior of MLCs. The chemical structure of the clays is characterized by the random isomorphic substitution of Al^{3+} by Mg^{2+} atoms and Si^{4+} by Al^{3+} atoms in the octahedral and the tetrahedral sheet, respectively. The isomorphic substitutions also obey Loewenstein's rule to avoid two adjacent substitutions. In the present study, four different types of mixed layers I-Mt clays were simulated that their chemical compositions and a charge per unit cell (uc) of them are shown in Table1, and the initial structures of the clay mineral layer are demonstrated in Fig. 1.

The supercell model of constructed I-Mt MLCs includes 4 clay sheets (two sheets each of illite and Mt), where each layer contains 5×4 unit cells. As an example, for the case of I (HC)-Mt (HC) with 20 unit cells, the model has 20 isomorphous substitutions of Al^{3+} by Mg^{2+} in the octahedral sheets of Mt. In the illite clay sheets, 4 Al^{3+} were replaced with Mg^{2+} in the octahedral sheet as well as replacement of 32 Si^{4+} with Al^{3+} in the tetrahedral sheet (16 in each tetrahedral sheet). To balance the generated negative charge of layers, according to the charge quantity, counterions were added into the interlayers. Therefore, 10 Na^+ and 18 K^+ were added between the interlayer of Mt-Mt and I-I interlayers, while the remaining cations were distributed between I-Mt clay interlayers.

2.2. Molecular dynamics simulation

All MD simulations were performed using GROMACS 5.1.2 Software [51]. To generate the molecular structure of MLCs, CLAYFF

Table 1
Chemical Compostion of Simulated MLCs.

Item	Type of MLC	Chemical Compositions		e.uc^{-1}
1	I (HC)-Mt (HC)	I	$K_{1.8}[Si_{6.4}Al_{1.6}][Al_{3.8}Mg_{0.2}]O_{20}(OH)_4$	−1.8
		Mt	$Na[Si_8][Al_3Mg]O_{20}(OH)_4$	−1.0
2	I (HC)-Mt (LC)	I	$K_{1.8}[Si_{6.4}Al_{1.6}][Al_{3.8}Mg_{0.2}]O_{20}(OH)_4$	−1.8
		Mt	$Na_{0.75}[Si_{7.75}Al_{0.25}][Al_{3.5}Mg_{0.5}]O_{20}(OH)_4$	−0.75
3	I (LC)-Mt (HC)	I	$K[Si_7Al][Al_4]O_{20}(OH)_4$	−1
		Mt	$Na[Si_8][Al_3Mg]O_{20}(OH)_4$	−1.0
4	I (LC)-Mt (LC)	I	$K[Si_7Al][Al_4]O_{20}(OH)_4$	−1.0
		Mt	$Na_{0.75}[Si_{7.75}Al_{0.25}][Al_{3.5}Mg_{0.5}]O_{20}(OH)_4$	−0.75

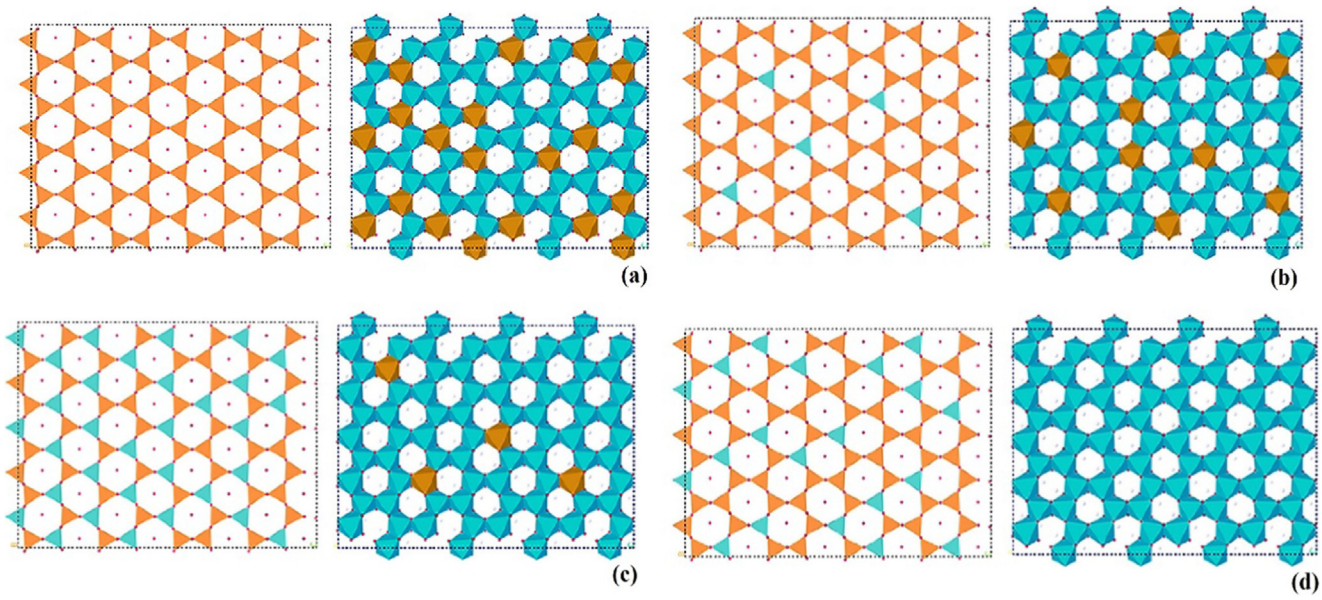

Fig. 1. Top view of the initial structures of clay mineral layer: (a) Mt (HC), (b) Mt (LC), (c) I (HC), and (d) I (LC). The left and the right sheets are tetrahedral and octahedral, respectively. Si^{4+}, Al^{3+}, and Mg^{2+} are colored as orange, blue, and brown.

forefield [52] was used in combination with the flexible point charge (SPC) model for modeling the interlayer water molecules [53]. In each simulation, the systems were minimized using the steepest descent method. After energy minimization, 2 ns MD simulations in an isothermal – isobaric ensemble (NPT) were conducted with the time step of 0.01 fs at the condition of T = 348 K and P = 130 bar [54]. Then, the equilibrated system was put into the additional 10 ns second of NPT with the time step of 1 fs at the same pressure and temperature conditions to calculate the basal spacing d-value of interlayers. At the final stage, 5 ns NVT simulations were conducted to achieve the equilibrated configurations. The density profile and the radial distribution function were calculated from the equilibrated configurations. In all simulations, the temperature and the pressure were controlled using a V-rescale thermostat [55] and isotropic Parrinello-Rahman algorithms [56], respectively. Periodic boundary conditions were imposed in three directions, and applying the semi-isotropic pressure allowed the system to freely expand the clay layers along the Z-axis (See Fig. 2). To calculate long-range electrostatic interaction, the particle-mesh Ewald (PME) summation method was applied with an accuracy of 10^{-4}. At the same time, the cut-off radius was adjusted 1.4 nm for both Van Der Waals (VDW) and electrostatic interactions.

In this study, 4 different I-Mt systems were simulated for 1 to 10 water molecules per unit cell, indicating monolayer the (1 W) and bilayer (2 W) hydration status of the MLCs. In general, 44 cases

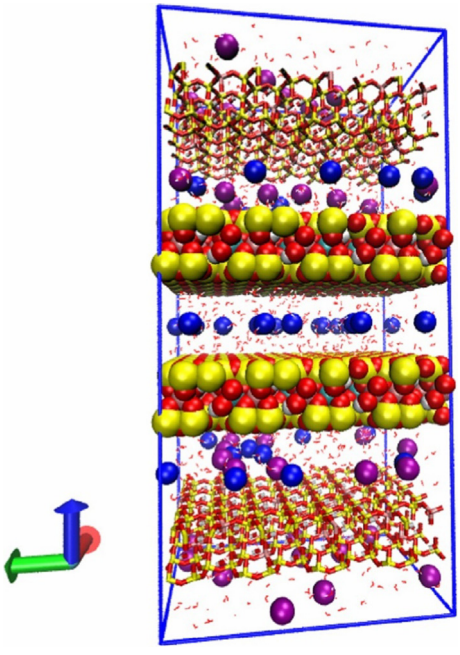

Fig. 2. The supercell structure of MLCs. Two middle layers are Mt and top and bottom layers are illite Si^{4+}, Al^{3+}, Mg^{2+}, K^+, Na^+, O^-, and H^+ are colored as yellow, gray, green, violet, blue, red, and white, respectively.

were simulated, and in all simulations, water molecules were randomly distributed in the interlayers after the distribution of counterions in the middle of interlayers.

3. Results

3.1. Swelling and basal spacing

The MLCs crystalline swelling process was characterized by the basal spacing d-value, defining as the distance between tops of two consecutive clay sheets for four different simulated systems as the function of water molecules entering the interlayer. In the crystalline swelling regime of clays, the interlayer's basal spacing d-value presents stepwise increases, which indicate the transition between two different hydrate states. First, in each hydration state, some of the adsorbed water molecules hydrate counterions and form the hydration shells. This step is the primary reason for the interlayer expansion. Following this step, water content fills the available remained space between interlayers in which minor interlayer expansion will result [46].

In this study, the pure Mt and illite interlayers' negative charge was only compensated by adding Na^+ and K^+, respectively. Moreover, due to the difference in the required number of cations - Na^+ ions and K^+ ions that we inserted between two I-Mt interlayers in I (HC)-Mt (LC) and I (LC)-Mt (LC) simulation systems, an interlayer with 7 Na^+ and 18 K^+ for I (HC)-Mt (LC) and 7 Na^+ and 10 K^+ for I (LC)-Mt (LC) were selected for analysis.

The d-values of pure Mt interlayer distance were consistent with previously published experimental values and simulated results [22,32,36]. The basal spacing d-value of pure illite interlayers was in good agreement with recently published research by Li et al.[37]. It should be noted that due to applying a range of charge densities and charge site locations in previous studies, slight differences in both simulated and experimental results are acceptable. Moreover, some of the small differences between the computed and experimental results may be incorporated into the overestimated surface-ion interaction for the surface oxygens in the CLAYFF force field.

Fig. 3a-d shows the group based on the absolute basal spacing of interlayers for four distinct systems. Moreover, for a better understanding of the swelling behavior of interlayers, the percentage of the relative increase in basal spacing of interlayers which are computed bases on their dry state, are presented in Fig. 3e-h.

In general observation, they demonstrated that (i) the general trends of the computed absolute basal spacing of interlayers in each system were relatively similar, (ii) the absolute basal spacing d-values of interlayers expanded similarly for both I (LC)-Mt (HC) and the I (LC)-Mt (LC) during 1 W and 2 W hydrate statues, however, the slight difference between the absolute d-values were observed for I (HC)-Mt (HC) and I (HC)-Mt (LC) in the presence of high water concentrations, (iii) considering the percentage of the relative increase in d-values of interlayers, Mt-Mt interlayer swelled the most compared to the other systems, (iv) in almost all cases, swelling of the I-Mt clay were analogous to the I-I. This revealed the dominant rule of K^+ in the swelling behavior of I-Mt. However, for the case of I (LC)-Mt (HC) and in comparison with I (HC)-Mt (HC), an increasing number of Na^+ in the presence of lower concentrations of K^+ gave rise to a higher basal spacing d-value of I-Mt interlayer. In what follows, we provide more in-depth insight into the observed swelling characteristic behavior of interlayers by considering the relative basal spacing d values.

Comparing the swelling curve of interlayers in Fig. 3e-h revealed that the order of swelling in the symmetric Mt-Mt interlayer was higher than other interlayers in all simulated MLCs. To understand the reasons behind the swelling behavior of systems, three factors of hydration enthalpy of the interlayer counterions, charge site locations, and charge quantity were considered for differences in the interlayer distance. As we know, the lower the hydration enthalpy of cations, the less interlayer swelling will result. Since Na^+ compared to K^+ has a higher hydration enthalpy-that is -406 and -320 kJ mol^{-1}, respectively, the presence of Na^+ leads to an increase in the interlayer distance as a result of the formation of a larger hydration shell. The difference in the basal spacing d-values of both the symmetric Mt-Mt and I-I was not restricted to only hydration enthalpy of counterions. Indeed, their structural differences in respect of the charge site location and charge amount also had a great influence on the interaction of the cations and clay surfaces. In more detail, the main negative charge of Mt clay sheets was due to octahedral substitutions of Al^{3+} with Mg^{2+}, however, illite sheets were more negatively charged on the tetrahedral ones. Differences between charge locations culminated in a more strong interaction of counterions with the illite surface. This is why the symmetric I-I interlayer had less tendency to swell compared to the Mt-Mt interlayer. Furthermore, in all cases, the I-Mt interlayers behaved fairly as similar to the I-I interlayers except in the I (LC)-Mt (HC). In this case, the basal spacing d-values were approximately the average interlayer distance values of I-I and Mt-Mt for each separated water content. The lower tetrahedral charge density of the illite sheet compared to the high octahedral charge density of the Mt clay sheet as well as the relative increase in Na^+ in comparison with K^+, may result in such swelling behavior.

In order to investigate the effect of the charge amounts and charge locations on the swelling behavior of interlayers, the relative basal spacing curves were grouped by the interlayer types in Fig. 4. First, we assessed the effect of charge amounts on the Mt-Mt and I-I interlayers' swelling behavior, which are octahedrally and tetrahedrally charged, respectively. Then, we look deep insight into the influence of both mentioned factors on the changes of I-Mt clay interlayer distance.

Fig. 4 indicates that the general trends in the basal spacing d-value of both Mt-Mt interlayers were similar. Also, hydration states of 1 W and 2 W and transition to them were manifest. At both high and low water contents, the highly charged Mt clay sheet swelled more compared to the slightly charged one. This is mainly due to the weak counterion-clay surface interactions and high hydration enthalpy of Na^+, which resulted in forming of fully hydrated ions. In fact, in the presence of more Na^+ between the Mt-Mt interlayer, more clay swelling was anticipated [29,37,46]. Also, Fig. 4 indicates that the overall transition was the same for both I-I interlayers. Regardless of the lower extension of the I-I interlayer compared to the Mt-Mt interlayer, the presence of K^+, as a low hydration enthalpy counterion between the I-I interlayer region led to monotonically swelling of the clay. As is shown, the more K^+ in the interlayer, the more smoothly changes happened while clay swelling. In addition, for highly charged illite clay sheets, the delay in transition was observed due to the high number of K^+ compared to the case with lower charge density and their interaction with tetrahedral sheets of illite. Considering the basal spacing d-value, during the first stage of hydration (1 W), the rate of changes in the basal spacing of highly charged illite was a bit larger than the other cases. However, at the compacted double layer water stage, the trend was reversed in which the illite with higher charge density showed less tendency to swell. In fact, high charge density on the tetrahedral sheet of the illite and the more number of K^+ were the major reasons for the less-swelling behavior of illite compared with Mt. As was mentioned, during the 1 W hydration state, illite with low charged density had less tendency to expand compared to the highly charged one. This means that presence of a lower number of K^+ leaded to such behavior. During the 2 W hydration state, however, the powerful interaction between K^+ with the highly

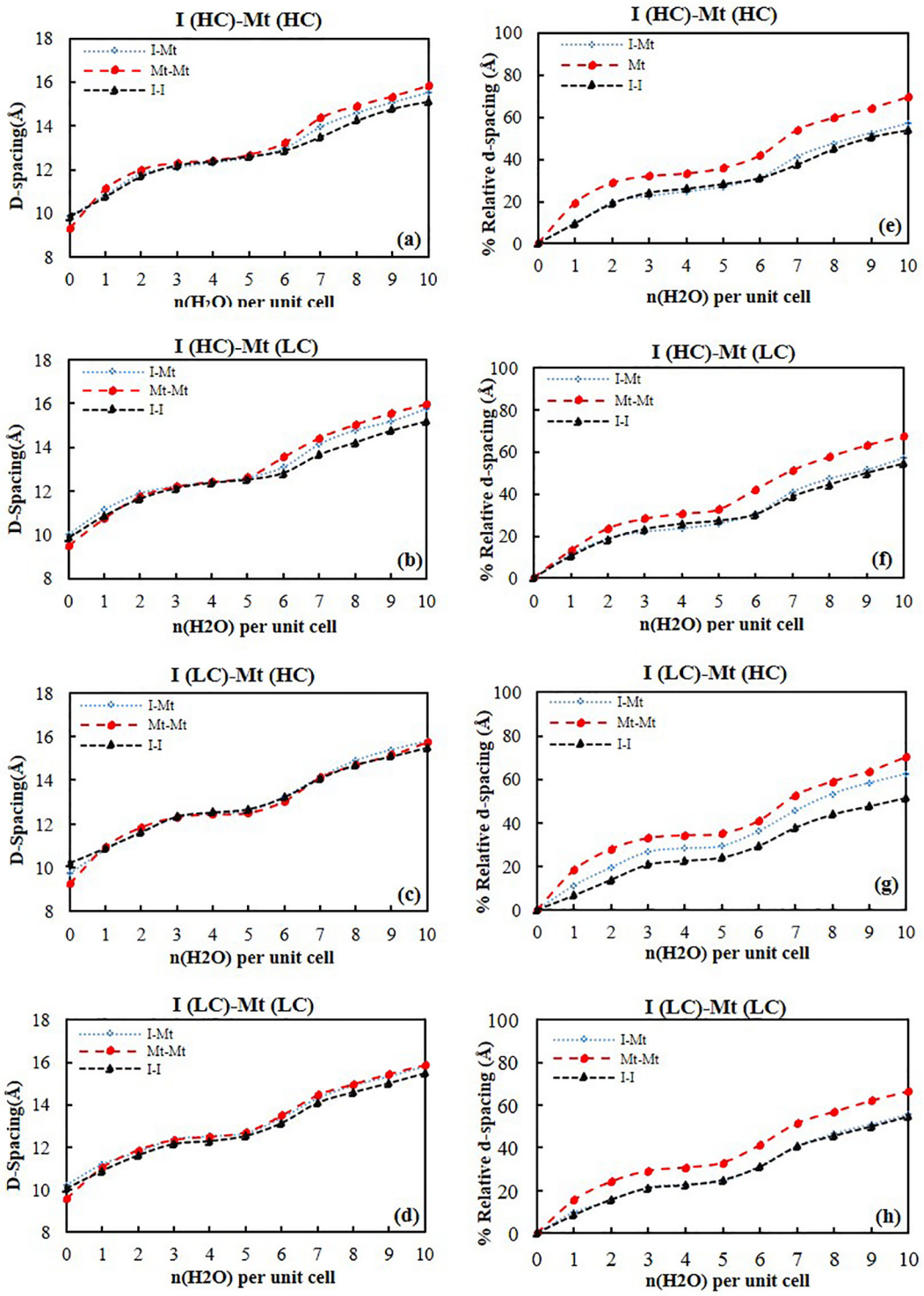

Fig. 3. The absolute (a-d) and relative (e-h) basal spacing value of the clay interlayers as a function of water contents, grouped by the charge amount and charge locations.

charged tetrahedral sheets was the major reason for the lower expansion of the interlayer in comparison with the low-charged one. It should be mentioned that the obtained information of I-I interlayer swelling tendency is consistent with the recently published paper by Li et al. [37].

Fig. 5a-f compares the relative basal spacing variation of I-Mt clay interlayer as a function of charge amounts and charge site locations. To better gain a detailed understanding of the differences between the basal spacing of I-Mt clay interlayers, we grouped the basal spacing curve of every two interlayers in a graph. In this regard, the following points are worth mentioning: (i) For the I-Mt clay interlayer in which illite had high charge density on the tetrahedral sheet, the swelling behavior of the I-Mt clay interlayer was reasonably independent of charge amounts of the Mt, which is octahedrally charged. (Fig. 5a), (ii) When the I-Mt clay interlayer had low tetrahedral charge density on the illite sheets, charge amounts of the Mt played a significant role in the swelling behavior of the interlayer. In more detail, the lower charge of illite

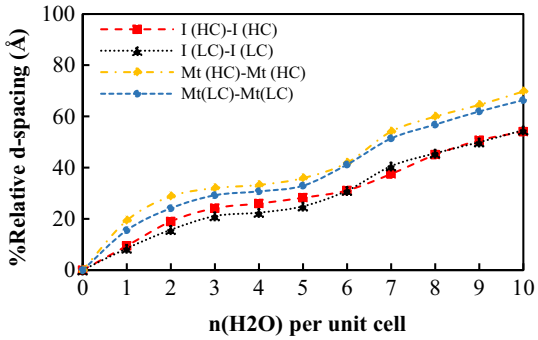

Fig. 4. Comparison of the relative basal spacing of Mt-Mt and I-I interlayers as a function of charge amounts.

sheets and the more charge of Mt sheets in the I-Mt clay interlayer resulted in higher swelling and distance of interlayer (Fig. 5b-c,f), (iii) The swelling behavior of a system including a high charge illite sheet, regardless of the charge amounts of Mt, was similar to the I-Mt clay interlayer. The reasons behind such behavior of I-Mt clay interlayers are related to the following key important facts. First, the identity of the interlayer's counterions. In mixed-ion MLCs, a high fraction of K^+ reduces the swelling tendency of interlayers. This is due to no powerful attraction between K^+ and water molecules. However, in the same fraction of K^+ and Na^+, the possibility of swelling behavior of clay increases [57]. Second, charge locations and charge amounts. When MLCs are more negatively charged on the tetrahedral sheet of illite, the interaction between counterions and surface sheet will increase, in which the possibility of their hydration is reduced, especially for Na^+. On the other hand, in the case of the low charge density of I-Mt clay, no serious hydration was observed due to fewer Na^+.

3.2. Atomic density profile

The distribution of interlayer cations and water molecules in the clay interlayers were quantified by the one-dimension atomic density profile for 1 W and 2 W hydrate states and are illustrated in Figs. 6–8. Comparison of the atomic density profiles of simulated systems give a better insight into the effect of charge locations and charge density on the interactions of counterions with the clay surface.

Fig. 6a-d present the symmetric Mt interlayer systems' density profiles with high charge and low charge density on the octahedral sheet of the clays. For both cases, in the 1 W hydrate state, Na^+

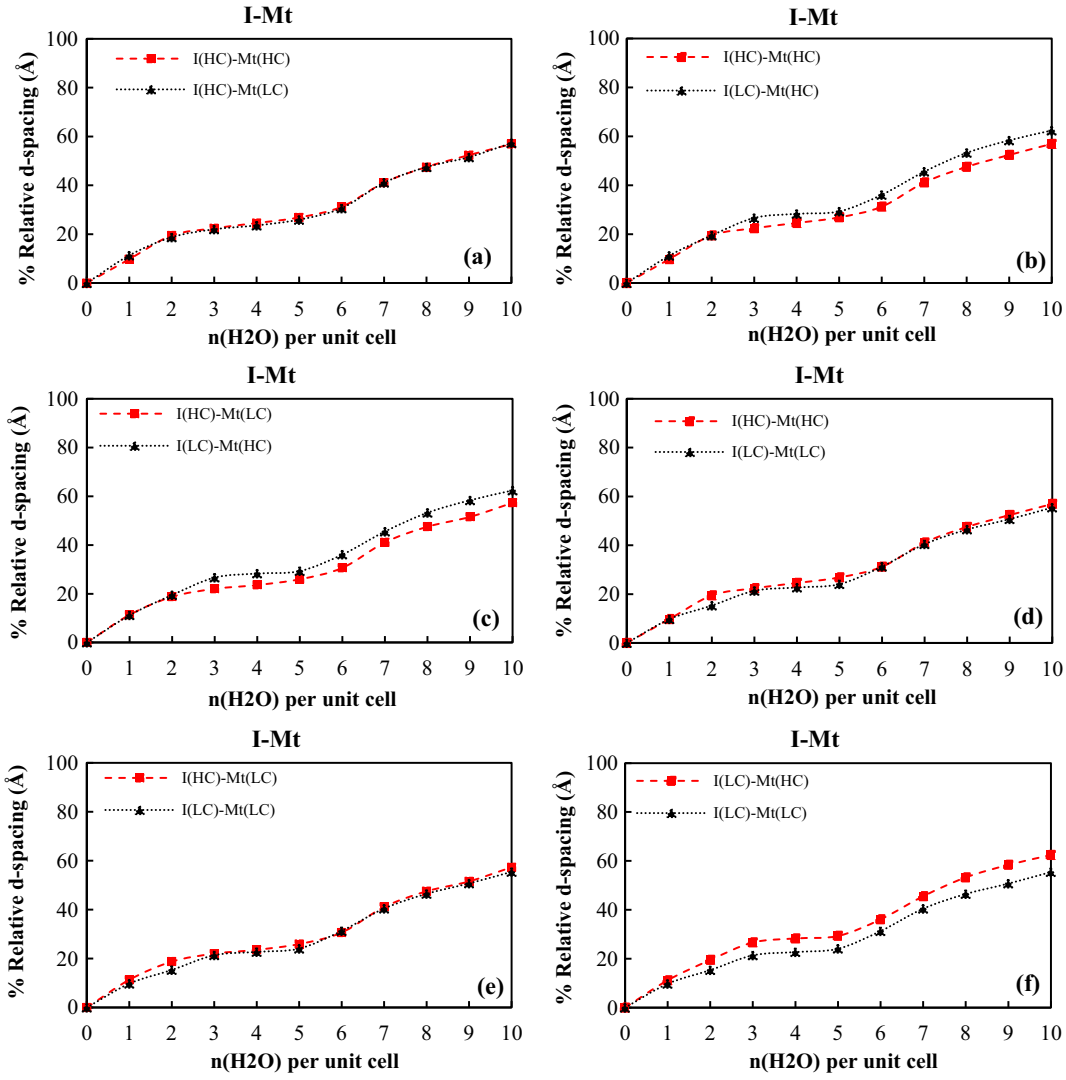

Fig. 5. Comparison of the relative basal spacing of the I-Mt interlayers as a function of charge amounts and charge locations.

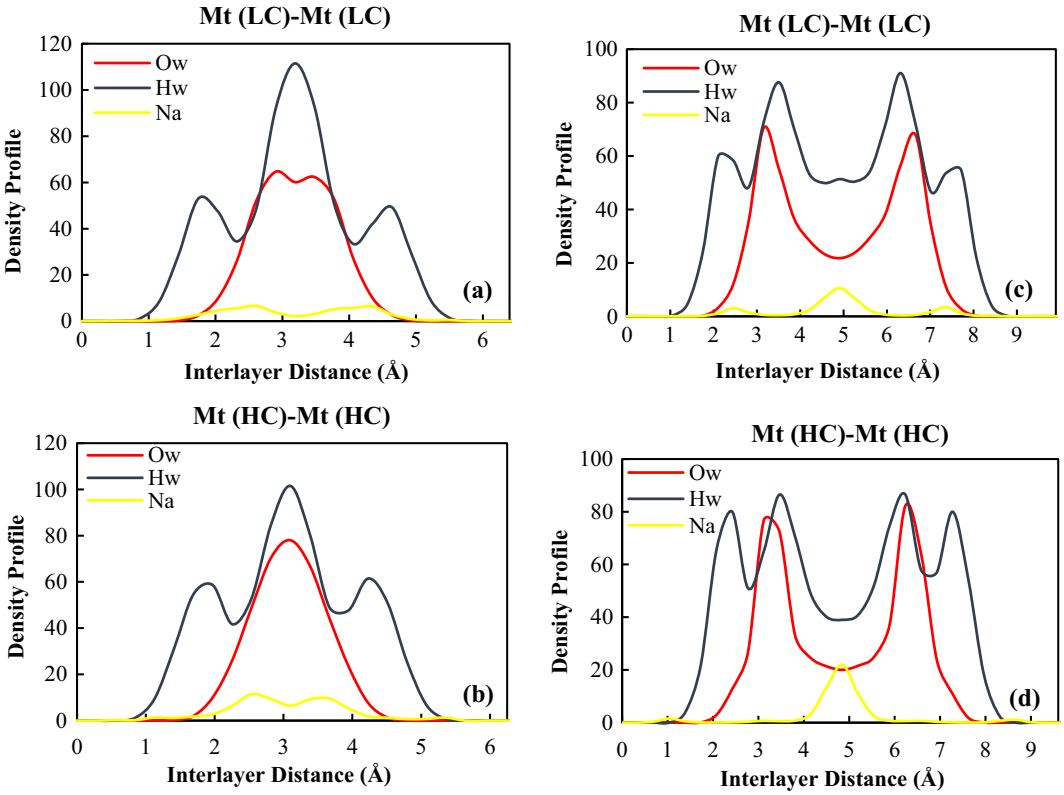

Fig. 6. Atomic density profiles of Na^+, O_w and H_w for the monolayer (a,b) and bilayer (c,d) hydrated low charged Mt (a,c) and high charged Mt (b,d). Water oxygen and hydrogen are represented by red and blue, and Na^+ by yellow.

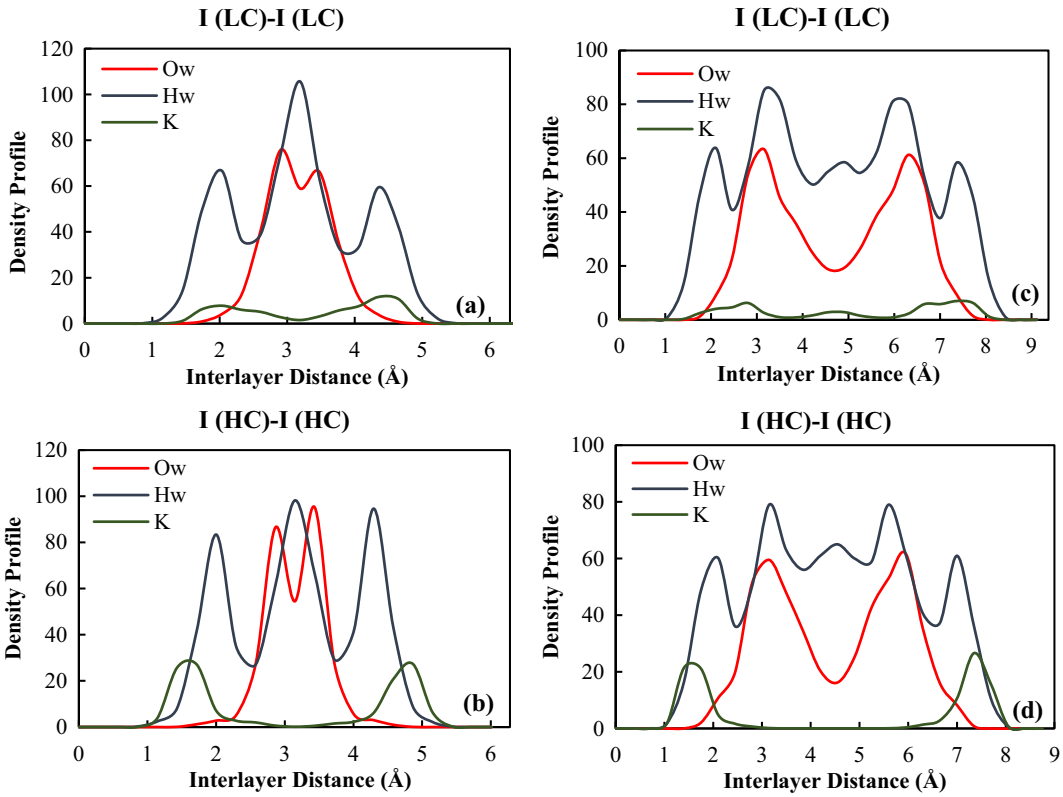

Fig. 7. Atomic density profiles of K^+, O_w, and H_w for the monolayer (a,b) and bilayer (c,d) hydrated low charged illite (a,c) and high charged illite (b,d). Water oxygen and hydrogen are represented by red and blue, and K^+ by green.

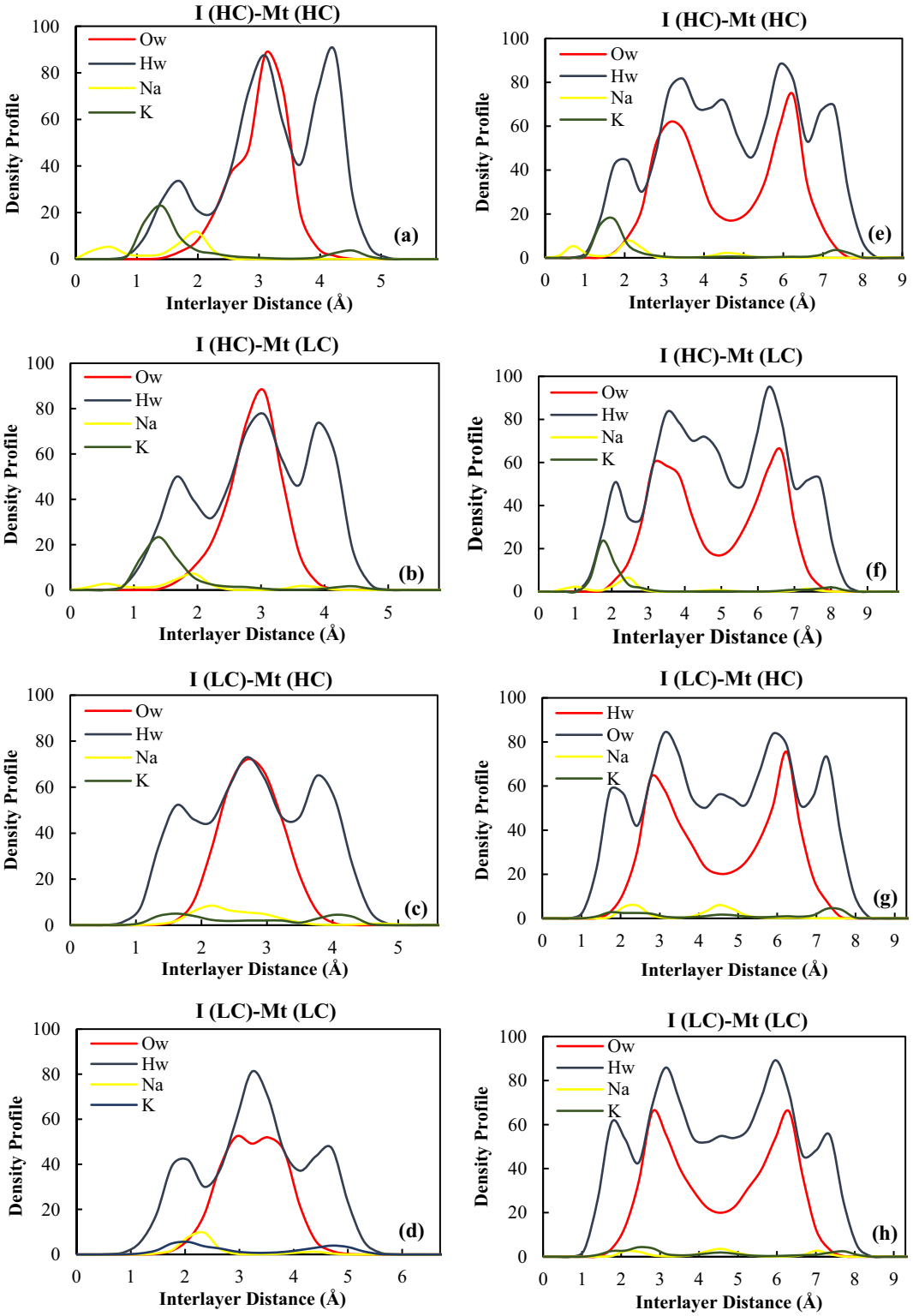

Fig. 8. Atomic density profiles of K^+,Na^+, O_w, and H_w for the monolayer (a-d) and bilayer (e,h) hydrated I (HC)-Mt (HC) (a,e), I (HC)-Mt (LC) (b,f), I (LC)-Mt (HC) (c,g), I (LC)-Mt (LC) (d,h), Water oxygen and hydrogen are represented by red and blue, and Na^+ and K^+ by yellow and green, respectively.

formed a broad peak with a shoulder near each clay surface. For the highly charged Mt, however, the shoulder was sharper, which indicated higher hydration and, as a result, more interlayer swelling. As the water content increased and the 2 W hydrate state formed, the broad centered profile of Na^+ was changed to a single peak at the midplane signifying the outer-sphere surface complex (OSSC). It should be noted that the shaper cation peaks in 2 W hydrate state of the high charge Mt was may be due to the imposed forces of water molecules on counterions to be transferred from clay surface to the center of interlayers, not because of higher hydration [47]. For the low charge Mt case, besides a single peak at the midplane, two small peaks near the clay surface represented the

inner-sphere surface complex (ISSC). This may be due to negative charge distribution on the tetrahedral layer and weakness of CLAFF force field, which overestimates surface oxygen-ion interaction. In the case of the high charge Mt in the 2 W hydrate state, two minor peaks were observed approximately less than 1.0 Å from surface oxygen atoms. This was due to unusual adsorption within ditrigonal cavities on the basal surface, so-called "anhydrous" [29]. It should be noted that the anhydrous ions were weakly detectable for the 1 W state of the high charge Mt.

Comparing the distribution of interlayer water molecules of Mt in Fig. 6.a-d revealed that in the case of 1 W hydrate state, the amount of charge density had no considerable influence on the water molecules distribution. On the other hand, in the 2 W hydrate state, an increase in charge density of the octahedral sheet resulting from the replacement of Al^{3+} with Mg^{2+} led to the presence of more hydrogen atoms of water near the oxygen on the clay's surface. Such interactions stemmed from the high polarization power of Mg^{2+} compared to the Al^{3+} ions. In the 2 W hydrate state, the oxygen peaks around central cations for both the low charge Mt and high charge Mt were relatively the same value indicating the cation hydration's similar tendency as previous analysis basal spacing d-value showed. The density profile of the Mt system was also consistent with the earlier studies [29,30,46,47].

The atomic density profile of the illite interlayer water molecules and K^+ are shown in Fig. 7a-d. At low charge density, the preference of the interlayer K^+ was forming the ISSC instead of the OSSC. For both 1 W and 2 W hydrate states, there was no sharp peak of cations in the midplane due to the low hydration enthalpy of K^+ (Fig. 7.a,c). That was why the low tetrahedrally charged illite had less tendency to swell. Moreover, another insight that proved the less-swelling behavior of this system was that hydration states did not influence the distribution of water molecules. In more detail, the water oxygen's prominent peak and the first peak of water hydration were virtually remained unchanged in different hydration states.

At high charge density, the two sharp peaks of K^+ near the clay surface exhibited strong interaction of the ions with the surface, which resulted in forming the ISSC. Such interaction was due to the high charge density of tetrahedral sheet and was the major reason for the less-swelling behavior of illite compared to Mt. Furthermore, in contrast to the Na^+-Mt system that adding water to the interlayer forced the Na^+ to move from hexagonal sites to the sites above the tetrahedral sheet, in high charge illite system, the distance of K^+ remained nearly unperturbed by increasing the water content. As similar to the low charge density, the interlayer water molecules' distribution was not changed when the hydration state was transformed to 1 W from 2 W. The water oxygen's prominent peaks and the first peak of water hydration approximately remained constant at 2.5 Å and 1.5 Å for 1 W and 2 W hydration states, respectively (Fig. 7b,d). The obtained results also agree well with the previous study [37].

Fig. 8a-f show the I-Mt clay interlayers' atomic distribution for the simulated systems with different charge locations and charge sites at the 1 W and 2 W hydrate states. As discussed in the previous section, two reasons for the lower hydration enthalpy of K^+ and high charge density on tetrahedral sheets of illite were considered as effective items on low basal spacing d-value of I-Mt clay interlayers. Considering the I (HC)-Mt (HC) and I (HC)-Mt (LC) interlayers, the atomic density profiles were relatively close to each other. Fig. 8a,b indicate that at 1 W hydrate state, the preference of counterions was forming strong bonds with clay surface instead of hydration with water molecules. In fact, the high charge density of the illite tetrahedral sheet was the major reason for the adsorption of the counterions onto the clay surface and ISSC formation. The effect of the charge density was such that the strong interaction of Na^+ with illite surface led to ions penetration in the ditrigonal cavities of the siloxane surface. This also suggested that the ditrigonal cavities were better fits for Na^+ than K^+ [37]. On the Mt side of the I (HC)-Mt (HC) interlayer, ISSC was only formed for and K^+, while their numbers were not comparable with the illite surface side. For the I (HC)-Mt (LC) interlayer, besides the ISSC of K^+, the small peak of Na^+ near the Mt side of the interlayer represented the ISSC. The difference in forming ISSC of Na^+ with Mt surface originated from various polarization power of Mg^{2+} in the octahedral sheet between the high charge Mt and low charge one. In more detail, comparing water molecules distribution of two discussed interlayers, Fig. 8a,b. indicate that water molecules preferred to establish strong hydrogen bonds with the Mt surface rather than the illite surface, which may be due to perturbable properties of K^+ and even high charge density of the Mt on the octahedral sheet. The fact is that the more octahedral substitution of Al^{3+} with Mg^{2+} in Mt clay, the shaper peak of the water hydrogen near the Mt surface will result. High polarization power Mg^{2+} compared to the Al^{3+} is responsible for the difference. Therefore, the more tendency of water molecules to be adsorbed on high charged Mt imposed force on Na^+ to transfer from near the Mt surface to the middle of the interlayer. On the other hand, the denser layer substitution of the illite adsorbed detached ions on its surface. That was why no Na^+ were present near the Mt surface to form the ISSC and almost all of the ions were concentrated near illite surface. As was shown in the previous section, in the 1 W hydration state, the swelling behavior of the I (HC)-Mt (HC) and I (HC)-Mt (LC) was analogous to illite as the less-swelling clay minerals.

In the 2 W hydrate state, interlayer molecules' distribution was generally similar for both simulated systems (Fig. 8e,f). A majority of K^+ were placed close to the illite surface and were attributed to the ISSC. The weaker peak of K^+ next to the Mt surface was also consistent with the ISSC. Because of the lower hydration enthalpy of K^+ and less tendency to hydrate, as well as strong interaction with the clay mineral surface, there was no peak in the midplane. As the water content increased, although most of the Na^+ remained close to the illite surface, some Na^+ appeared at the midplane of the interlayer ascribing to the OSSC and cation hydration. As discussed in Section 3.1, the same swelling behavior was seen in the case of I (HC)-Mt (HC) and I (HC)-Mt (LC) for 2 W hydrate state in which increases in water content caused the slight increase in interlayer distance compared to the illite. The OSSC of Na^+ in I-Mt clay clarified the difference in the basal spacing d-values of studied systems. Moreover, as similar to the 1 W hydration state, ISSC of Na^+ with Mt surface was only formed when the charge of Mt was low, and water molecules tended to be adsorbed by the Mt surface rather than illite, especially for the highly charged Mt.

Fig. 8c,d,g,h demonstrate the atomic distribution in I-Mt where the Mt has variable charge densities while illite has low charge density on the tetrahedral sheet. The results manifested significant differences with the two described cases, which included the highly charged illite. As is clear, the distribution of atoms depends on the layer charge density of clays. In the case of the high charge illite, most of the atoms preferred to have strong interaction with a clay surface. On the other hand, it seems that when the system included the low-charge illite, hydration enthalpy of counterions played major role in the swelling behavior of the system. Fig. 8c shows that the interlayer Na^+ were mainly presented in the middle of the interlayer with a relative tendency towards the illite surface at the 1 W hydrate state. While the majority of Na^+ were distributed near the illite surface rather than the midplane for the I (LC)-Mt (LC) interlayer at 1 W hydrate state. That contributed to more swelling of the I (LC)-Mt (HC) interlayer. Comparing the interlayer K^+ distribution, most of the K^+ formed ISSC near both sides of the clay surface instead of creating the OSSC (Fig. 8c,d). This is mainly related to their low hydration enthalpy. In addition,

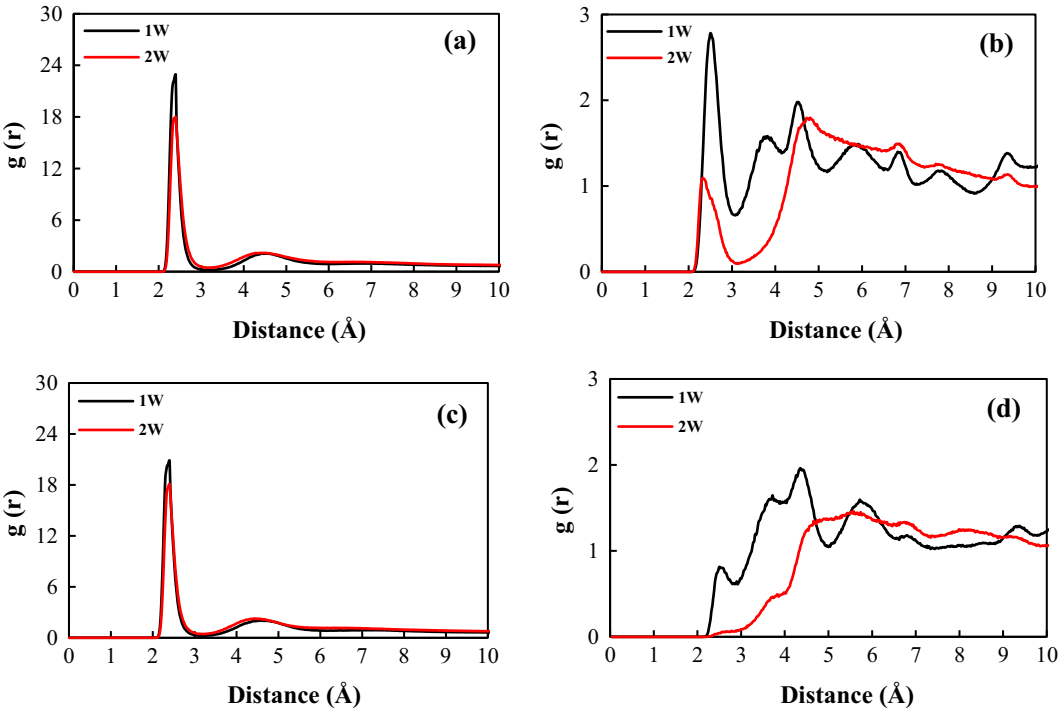

Fig. 9. RDF for Na^+-O_W and Na^+-O_s at monolayer hydrate state (black) and bilayer hydrate state (red), Mt (HC)- Mt (HC) (a,b) and Mt (LC)-Mt (LC) (c,d).

similar to the previous cases we studied, the preference of the water molecule had hydrogen bonds with Mt surface, as the shaper peak of hydrogen was shown (Fig. 8c,d.).

In the 2 W hydrate state of I (LC)-Mt (LC) and I (LC)-Mt (HC), the distribution of ions was relatively analogous to each other (Fig. 8g,h). For both K^+ and Na^+ in the I (LC)-Mt (LC) interlayer, the presence of two peaks near clay surfaces and a single peak at the midplane indicated ISSC and OSSC, respectively. In the I (LC)-Mt (HC) interlayer, although K^+ were distributed as similar as the former case, Na^+ formed a relatively sharp peak at the midplane and ISSC near the illite surface with no interaction to the Mt surface. As was mentioned, the higher tendency of water molecules to the high charge Mt surface pushed the Na^+ to the middle of the interlayer. In addition, due to the low charge density of illite on the tetrahedral sheet, no strong interactions were observed so as to adsorb these detached ions. As a result, more Na^+ were hydrated by water molecules that culminated in more swelling.

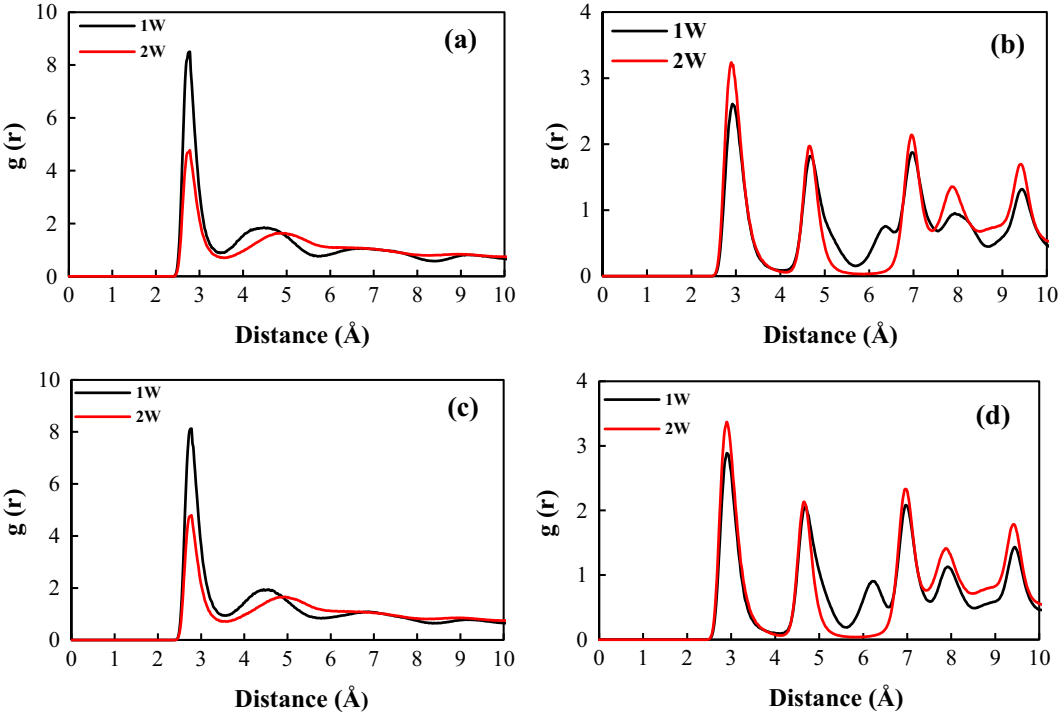

Fig. 10. RDF for K^+-O_W and K^+-O_s at monolayer hydrate state (black) and bilayer hydrate state (red), I (HC)- I (HC) (a,b) and I (LC)- I (LC) (c,d).

3.3. Radial distribution functions

Interaction between interlayer ions and water/surface of clay sheet was explored by calculating RDF g(r) of Na^+-O_w/O_s and K^+-O_w/O_s in the Mt-Mt, I-I, and I-Mt with various charge density and charge location. In this analysis, the surface oxygen atom of a clay sheet and a water oxygen atom are symbolized by O_s and O_w, respectively. In all simulated cases, regardless of variations in charge density, the main peak location of Na^+-O_w and K^+-O_w attributing to the first hydration shell appear at about 2.4 Å and 2.78 Å, respectively, which agree with previous studies [57-59].

Fig. 9 demonstrates the RDFs for the Mt-Mt systems. The height of the peak of Na^+-O_s for Mt (HC)-Mt (HC) was higher than the low charged Mt. This may be interpreted that the highly charged Mt attracted more Na^+ towards the clay surface, however, this was mainly due to the presence of more Na^+. Also, an increase in water content that led to significant changes in the location of Na^+ from the surface to midplane of the interlayer for both types of Mt confirmed it. As was mentioned, the higher number of counterions gives rise to more swelling. That is why the Mt-Mt with more charge experience more expansion.

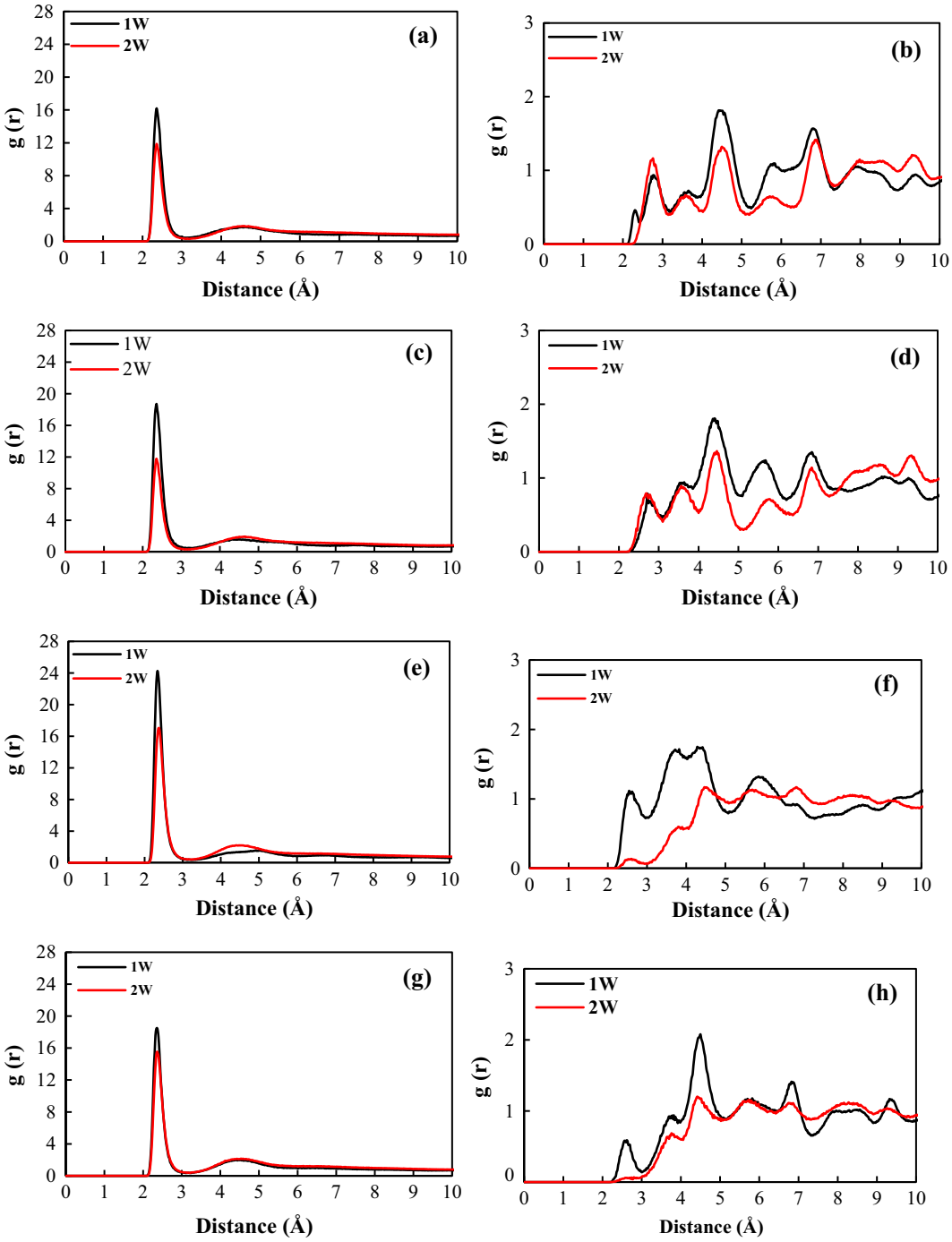

Fig. 11. RDF for Na^+-O_W and Na^+-O_s at monolayer hydrate state (black) and bilayer hydrate state (red), I (HC)-Mt (HC) (a,b), I (HC)-Mt (LC) (c,d), I (LC)-Mt (HC) (e,f), and I (LC)-Mt (LC) (g,h).

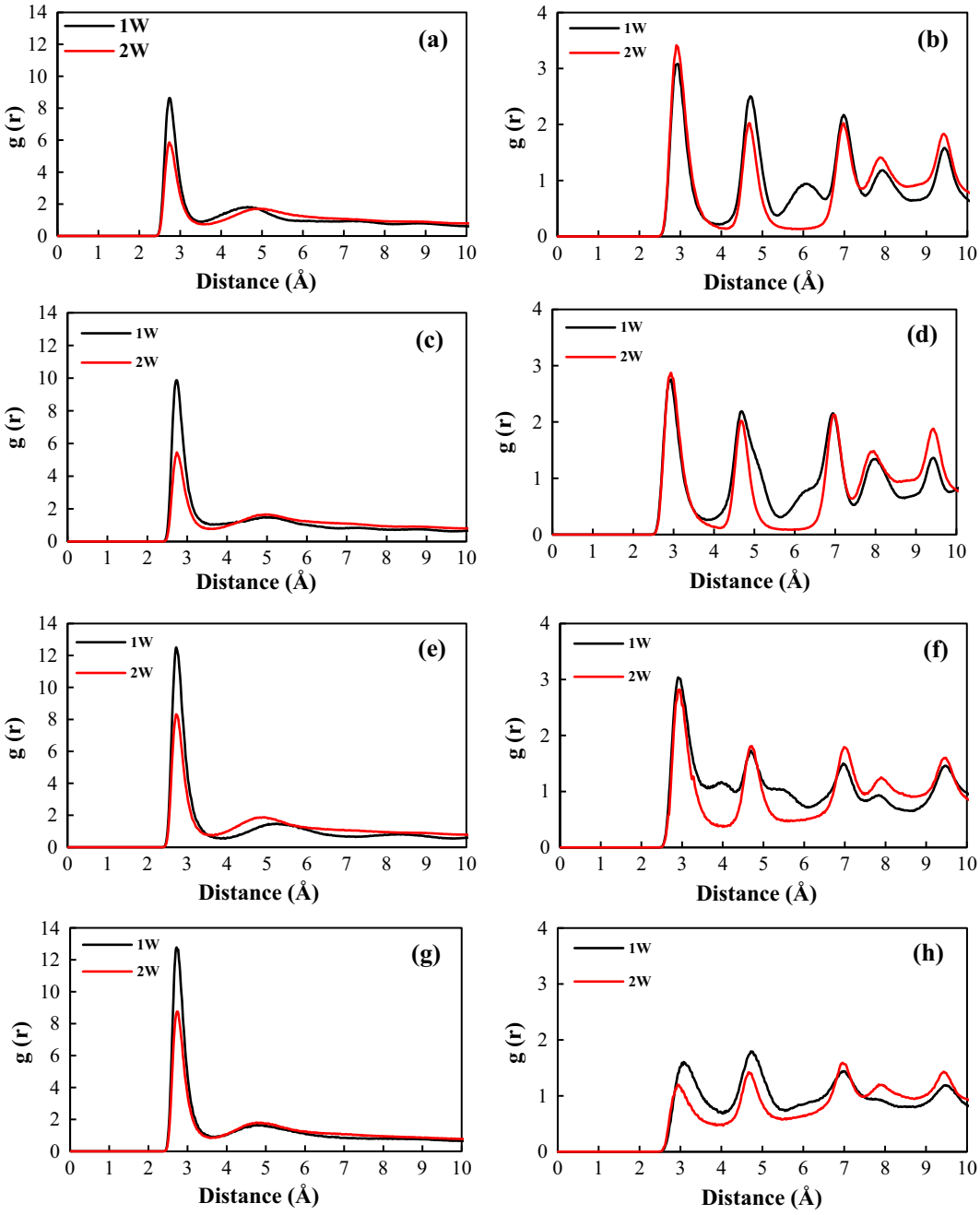

Fig. 12. RDF for K^+-O_W and Na^+-O_s at monolayer hydrate state (black) and bilayer hydrate state (red), I (HC)-Mt (HC) (a,b), I (HC)-Mt (LC) (c,d), I (LC)-Mt (HC) (e,f), and I (LC)-Mt (LC) (g,h). (For interpretation of the references to colour in this figure legend, the reader is referred to the web version of this article.)

Fig. 10 also presents the RDF value of K^+-O_w/O_s in I-I systems. Owing to the low hydration enthalpy of K^+, the value of $r_{k\text{-}Os/Ow}$ was considerably lower than $r_{Na\text{-}Os/Ow}$. In addition, the RDFs of $r_{k\text{-}Os}$ confirmed the results of both basal spacing d-values and profile density of I-I. When water content increased, no K^+ migrated to the middle of the illite clay interlayer. Indeed, low hydration enthalpy of K^+ as well as tetrahedrally charged of illite were the reasons of the less-swelling behavior of illite compared to Mt.

Fig. 11 presents the RDFs of the Na^+-O_w/O_s in I-Mt clays with different charge densities and charge site locations. In all cases, the gradual increase in water content between interlayers gave rise to a decrease in the intensity of the main peaks of Na^+-O_w. As is shown, the highest central peak Na^+-O_w was for the I (LC)-Mt (HC) case, which was in agreement with previous results indicating the great swelling behavior of the MLCs. Considering the RDFs values of Na^+-O_s, as water content increased in which monolayer hydrate state was changed to bilayer one, in general, a decrease in the height of peak indicated moving interlayer counterions towards the midplane of the interlayer. It should be noted that ions immigration behavior was not the same and was dependent on the charge density of clay sheet, which affected counterions-clay surface interaction. The results revealed that the presence of the high charge illite in the MLCs, most of the Na^+ with ISSC prefer to remain near the clay surface. This is due to the strong adsorption of the Na^+ on the clay sheet and an "anhydrous" behavior. In addition, the interesting obtained result was that in the I (HC)-Mt (HC), the first main peak of Na^+-O_s for the bilayer hydrate state was higher compared to the monolayer one. This significant increase was mostly

due to the adsorption of Na^+ to illite clay sheets, which were detached through the pushing force of water molecules that had a strong tendency towards clay surface and hydrogen bonds formation (Fig. 11b). Moreover, considerable changes in the location of interlayer ions in the I (LC)-Mt (HC) when water molecules increased confirmed the high swelling behavior of this system. For the I (LC)-Mt (LC) case, a decrease in the height of peak location was also evident at the 2 W hydrate state in comparison with the monolayer one. However, the major reason for interlayer reluctance to expand was the fewer number of Na^+ in the presence of K^+.

Fig. 12 also indicates the RDFs of the K^+-O_w/O_s in I-Mt. The RDF value of K^+-O_w decreased as the water content increased. Needless to say that the main peak of K^+-O_w for all four simulated cases was lower than Na^+-O_w peaks because K^+ was reluctant to fully hydrate. Furthermore, comparing the height of K^+-O_w showed that when MLCs include high charge illite, the order of $r_{cation\text{-}Ow}$ was lower than the case with low charge illite. This is mainly due to strong cation-illite surface interaction. The RDFs of the K^+-O_s revealed no significant changes in the location of K^+, as the hydration state was changed to bilayer from monolayer. The reluctance of K^+ to move towards the midplane was not only due to lower hydration enthalpy of the countetions but due to the presence of high charge clay sheet in the MLC, as well. In the presence of no high-charge clay sheet, some of the counterions immigrated to the midplane as water content increased (Fig. 11h). However, the reluctance of K^+ to hydrate resulted in lower interlayer expansion.

4. Summary

The present work investigated the crystalline swelling behavior of K^+-I-Na^+-Mt with different layer charges by using molecular dynamics simulation. Through a comparison of four different I-Mt clay systems with various charge amounts and charge distribution and simultaneous analysis of the basal spacing d-values, density profile, and RDFs to have a precise interpretation of systems, we observed subtle points in the crystalline swelling behavior of I-Mt structures. In the presence of highly tetrahedral charged illite in the I-Mt clay, regardless of the octahedral sheet charge quantity of Mt, the crystalline swelling behavior of the MLCs followed the swelling behavior of illite. However, the charge distribution of the Mt played pivotal roles in the swelling of the MLCs when the system included low-charged illite or the Mt and illite have the same charge density. In addition to the charge distribution of the MLCs, the counterion hydration effect can also be considered a critical factor in the interlayer expansion of MLCs. Indeed, I-Mt clays with low charged illite were highly affected by the hydration effect. In the case of a low tetrahedral charge of illite, an increase in Na+ in respect of K+ changed the swelling behavior of I-Mt clay towards following Mt swelling behavior. However, the strong interaction of Na^+ with highly tetrahedral charged of illite in I-Mt clay minimized the hydration effect. Furthermore, the I-Mt system, including Mt with highly octahedral charged sheet and illite with low charge density increased polarization of water molecules leading to adsorption of water molecules near the Mt clay surface. This affected the polarization of the other atoms, and as a result of water molecule adsorption, Na^+ immigrated into the midplane of the structure and started hydration. This increased the interlayer distance of the I-Mt clay system. Such behavior revealed how the Mt octahedral substitutions have a significant influence on clay swelling. Overall, besides charge quantity, both tetrahedral and octahedral substitution greatly influence the interlayer expansion of clay systems.

Declaration of Competing Interest

The author declare that there is no conflict of interest.

References

[1] B.B. Velde, A. Meunier, The origin of clay minerals in soils and weathered rocks, Springer Science & Business Media, 2008.
[2] A. Kausar, M. Iqbal, A. Javed, K. Aftab, H.N. Bhatti, S. Nouren, Dyes adsorption using clay and modified clay: a review, J. Mol. Liq. 256 (2018) 395–407.
[3] V.B. Yadav, R. Gadi, S. Kalra, Clay based nanocomposites for removal of heavy metals from water: a review, J. Environ. Manage. 232 (2019) 803–817.
[4] A. Sharma, S. Namsani, J.K. Singh, Molecular simulation of shale gas adsorption and diffusion in inorganic nanopores, Mol. Simul. 41 (5–6) (2015) 414–422.
[5] S. Zhan, Y. Su, Z. Jin, W. Wang, M. Cai, L. Li, Y. Hao, Molecular insight into the boundary conditions of water flow in clay nanopores, J. Mol. Liq. (2020) 113292.
[6] S. Li, C. Wang, X. Xu, L. Shi, N. Yin, Experimental and statistical studies on the thermal properties of frozen clay in Qinghai-Tibet Plateau, Appl. Clay Sci. 177 (2019) 1–11.
[7] J. Wang, Z. Chen, D. Shao, Y. Li, Z. Xu, C. Cheng, A.M. Asiri, H.M. Marwani, S. Hu, Adsorption of U (VI) on bentonite in simulation environmental conditions, J. Mol. Liq. 242 (2017) 678–684.
[8] P. Sellin, O.X. Leupin, The use of clay as an engineered barrier in radioactive-waste management–a review, Clays Clay Miner. 61 (6) (2013) 477–498.
[9] Z. Ma, R.P. Gamage, T. Rathnaweera, L. Kong, Review of application of molecular dynamic simulations in geological high-level radioactive waste disposal, Appl. Clay Sci. 168 (2019) 436–449.
[10] G.G. Machado, S.N. Guilhen, V.V. Krupskaya, S.V. Zakusin, E.A. Tyupina, J. Harada, R. Vicente, R.P.D. SOUZA, L.G.D. ARAUJO, D.C. Espinosa, Brazilian clays as potential buffer materials for radioactive waste final storage, 2020.
[11] A. Vaccari, Preparation and catalytic properties of cationic and anionic clays, Catal. Today 41 (1–3) (1998) 53–71.
[12] S.M. Dal Bosco, M. Gonçalves, F.C. Figueiredo, T. Galhardo, W.A. Carvalho, Sulfated pillared clay as catalyst in glycerol esterification with caprylic acid, Waste Biomass Valorization 7 (5) (2016) 1279–1288.
[13] Z. Hajizadeh, K. Valadi, R. Taheri-Ledari, A. Maleki, Convenient Cr (VI) Removal from Aqueous Samples: Executed by a Promising Clay-Based Catalytic System, Magnetized by Fe3O4 Nanoparticles and Functionalized with Humic Acid, ChemistrySelect 5 (8) (2020) 2441–2448.
[14] M.I. Carretero, M. Pozo, Clay and non-clay minerals in the pharmaceutical and cosmetic industries Part II. Active ingredients, Appl. Clay Sci. 47 (3–4) (2010) 171–181.
[15] M. Jafarbeglou, M. Abdouss, A.M. Shoushtari, M. Jafarbeglou, Clay nanocomposites as engineered drug delivery systems, RSC Adv. 6 (55) (2016) 50002–50016.
[16] K. Saha, K. Dutta, A. Basu, A. Adhikari, D. Chattopadhyay, P. Sarkar, Controlled delivery of tetracycline hydrochloride intercalated into smectite clay using polyurethane nanofibrous membrane for wound healing application, Nano-Structures & Nano-Objects 21 (2020) 100418.
[17] H. Zhong, Z. Qiu, D. Sun, D. Zhang, W. Huang, Inhibitive properties comparison of different polyetheramines in water-based drling fluid, J. Nat. Gas Sci. Eng. 26 (2015) 99–107.
[18] A. Moslemizadeh, S.K.Y. Aghdam, K. Shahbazi, S. Zendehboudi, A triterpenoid saponin as an environmental friendly and biodegradable clay swelling inhibitor, J. Mol. Liq. 247 (2017) 269–280.
[19] M. Ghasemi, A. Moslemizadeh, K. Shahbazi, O. Mohammadzadeh, S. Zendehboudi, S. Jafari, Primary evaluation of a natural surfactant for inhibiting clay swelling, J. Petrol. Sci. Eng. 178 (2019) 878–891.
[20] S.K.Y. Aghdam, A. Moslemizadeh, M. Madani, M. Ghasemi, K. Shahbazi, M.K. Moraveji, Mechanistic assessment of Seidlitzia Rosmarinus-derived surfactant for restraining shale hydration: a comprehensive experimental investigation, Chem. Eng. Res. Des. 147 (2019) 570–578.
[21] S.R. Shadizadeh, A. Moslemizadeh, A.S. Dezaki, A novel nonionic surfactant for inhibiting shale hydration, Appl. Clay Sci. 118 (2015) 74–86.
[22] R.W. Mooney, A.G. Keenan, L.A. Wood, Adsorption of water vapor by montmorillonite. II. Effect of exchangeable ions and lattice swelling as measured by X-ray diffraction, J. Am. Chem. Soc. 74 (6) (1952) 1371–1374.
[23] K. Norrish, J.P. Quirk, Crystalline swelling of montmorillonite: Use of electrolytes to control swelling, Nature 173 (4397) (1954) 255–256.
[24] E.S. Boek, P.V. Coveney, N.T. Skipper, Monte Carlo molecular modeling studies of hydrated Li-, Na-, and K-smectites: understanding the role of potassium as a clay swelling inhibitor, J. Am. Chem. Soc. 117 (50) (1995) 12608–12617.
[25] M.L. Nehdi, Clay in cement-based materials: critical overview of state-of-the-art, Constr. Build. Mater. 51 (2014) 372–382.
[26] B. Dazas, B. Lanson, A. Delvle, J.L. Robert, S. Komarneni, L.J. Michot, E. Ferrage, Influence of tetrahedral layer charge on the organization of interlayer water and ions in synthetic Na-saturated smectites, J. Phys. Chem. C 119 (8) (2015) 4158–4172.

[27] L. Sun, C.Y. Ling, L.P. Lavikainen, J.T. Hirvi, S. Kasa, T.A. Pakkanen, Influence of layer charge and charge location on the swelling pressure of dioctahedral smectites, Chem. Phys. 473 (2016) 40–45.
[28] J.K. Fink, Petroleum Engineer's Guide to Oil Field Chemicals and Fluids, 2012, 1, 1–42.
[29] S.L. Teich-McGoldrick, J.A. Greathouse, C.F. Jove-Colon, R.T. Cygan, Swelling properties of montmorillonite and beidellite clay minerals from molecular simulation: comparison of temperature, interlayer cation, and charge location effects, J. Phys. Chem. C 119 (36) (2015) 20880–20891.
[30] W.B.F. Ngouana, A.G. Kalinichev, Structural arrangements of isomorphic substitutions in smectites: molecular simulation of the swelling properties, interlayer structure, and dynamics of hydrated Cs–montmorillonite revisited with new clay models, J. Phys. Chem. C 118(24) (2014) 12758–12773.
[31] J. Qiu, G. Li, D. Liu, S. Jiang, G. Wang, P. Chen, X. Zhu, X. Cao, X. Lyu, Effect of layer charge characteristics on the distribution characteristics of H2O and Ca2 + in Ca-montmorillonites interlayer space: Molecular dynamics simulation, Materials 12 (14) (2019) 2318.
[32] A. Meleshyn, C. Bunnenberg, Swelling of Na/ Mg-montmorillonites and hydration of interlayer cations: a Monte Carlo study, J. Chem. Phys. 123 (7) (2005) 074706.
[33] D.A. Young, D.E. Smith, Simulations of clay mineral swelling and hydration: dependence upon interlayer ion size and charge, J. Phys. Chem. B 104 (39) (2000) 9163–9170.
[34] F.R.C. Chang, N.T. Skipper, G. Sposito, Monte Carlo and molecular dynamics simulations of electrical double-layer structure in potassium–montmorillonite hydrates, Langmuir 14 (5) (1998) 1201–1207.
[35] A. Chatterjee, T. Ebina, Y. Onodera, F. Mizukami, Effect of exchangeable cation on the swelling property of 2: 1 dioctahedral smectite—a periodic first principle study, J. Chem. Phys. 120 (7) (2004) 3414–3424.
[36] X.D. Liu, X.C. Lu, A thermodynamic understanding of clay-swelling inhibition by potassium ions, Angew. Chem. Int. Ed. 45 (38) (2006) 6300–6303.
[37] X. Li, Q. Li, S. Yang, G. Yang, Swelling of clay minerals: dual characteristics of K^+ ions and exploration of critical influencing factors, PCCP 21 (4) (2019) 1963–1971.
[38] M. Chávez-Páez, L. DePablo, J.J. DePablo, Monte Carlo simulations of Ca–montmorillonite hydrates, J. Chem. Phys. 114 (24) (2001) 10948–10953.
[39] D.E. Smith, Y. Wang, H.D. Whitley, Molecular simulations of hydration and swelling in clay minerals, Fluid Phase Equilib. 222 (2004) 189–194.
[40] M.D. Foster, Geochemical studies of clay minerals: II—relation between ionic substitution and swelling in montmorillonites, Am. Mineral.: J. Earth Planetary Mater. 38 (11–12) (1953) 994–1006.
[41] A. Seppälä, E. Puhakka, M. Olin, Effect of layer charge on the crystalline swelling of Na+, K+ and Ca2+ montmorillonites: DFT and molecular dynamics studies, Clay Miner. 51 (2) (2016) 197–211.
[42] L. Sun, The Effects of Structural and Environmental Factors on the Swelling Behavior of Montmorillonite-Beidellite Smectites: a Molecular Dynamics Approach. University of Eastern Finland Faculty of Science and Forestry Department of Chemistry Dissertation, 2016.
[43] J.A. Greathouse, R.T. Cygan, J.T. Fredrich, G.R. Jerauld, Molecular dynamics simulation of diffusion and electrical conductivity in montmorillonite interlayers, J. Phys. Chem. C 120 (3) (2016) 1640–1649.
[44] N.T. Skipper, F.R.C. Chang, G. Sposito, Monte Carlo simulation of interlayer molecular structure in swelling clay minerals 1. Methodology, Clays Clay Miner. 43 (3) (1995) 285–293.
[45] E. Ferrage, B. Lanson, L.J. Michot, J.L. Robert, Hydration properties and interlayer organization of water and ions in synthetic Na-smectite with tetrahedral layer charge. Part 1. Results from X-ray diffraction profile modeling, J. Phys. Chem. C 114 (10) (2010) 4515–4526.
[46] M. Rahromostaqim, M. Sahimi, Molecular dynamics simulation of hydration and swelling of mixed-layer clays, J. Phys. Chem. C 122 (26) (2018) 14631–14639.
[47] M. Rahromostaqim, M. Sahimi, Molecular dynamics study of the effect of layer charge and interlayer cations on swelling of mixed-layer chlorite-montmorillonite clays, J. Phys. Chem. C 124 (4) (2020) 2553–2561.
[48] C.E. Weaver, The distribution and identification of mixed-layer clays in sedimentary rocks, Am. Mineral.: J. Earth Planet. Mater. 41 (3–4) (1956) 202–221.
[49] R.C. Reynolds, J. Hower, The nature of interlayering in mixed-layer Illite-montmorillonites, Clays Clay Miner. 18 (1) (1970) 25–36.
[50] J.H. Lee, S. Guggenheim, Single crystal X-ray refinement of pyrophyllite-1 Tc, Am. Mineral. 66 (3–4) (1981) 350–357.
[51] D. Van Der Spoel, E. Lindahl, B. Hess, G. Groenhof, A.E. Mark, H.J. Berendsen, GROMACS: fast, flexible, and free, J. Comput. Chem. 26 (16) (2005) 1701–1718.
[52] R.T. Cygan, J.J. Liang, A.G. Kalinichev, Molecular models of hydroxide, oxyhydroxide, and clay phases and the development of a general force field, J. Phys. Chem. B 108 (4) (2004) 1255–1266.
[53] T.I. Mizan, P.E. Savage, R.M. Ziff, Comparison of rigid and flexible simple point charge water models at supercritical conditions, J. Comput. Chem. 17 (15) (1996) 1757–1770.
[54] V.N. Romanov, Evidence of irreversible CO2 intercalation in montmorillonite, Int. J. Greenhouse Gas Control 14 (2013) 220–226.
[55] G. Bussi, D. Donadio, M. Parrinello, Canonical sampling through velocity rescaling, J. Chem. Phys. 126 (1) (2007) 014101.
[56] S. Nosé, M.L. Klein, Constant pressure molecular dynamics for molecular systems, Mol. Phys. 50 (5) (1983) 1055–1076.
[57] J.H. Denis, M.J. Keall, P.L. Hall, G.H. Meeten, Influence of potassium concentration on the swelling and compaction of mixed (Na, K) ion-exchanged montmorillonite, Clay Miner. 26 (2) (1991) 255–268.
[58] V. Marry, P. Turq, T. Cartaler, D. Levesque, Microscopic simulation of structure and dynamics of water and counterions in a monohydrated montmorillonite, J. Chem. Phys. 117 (7) (2002) 3454–3463.
[59] P. Boulet, P.V. Coveney, S. Stackhouse, Simulation of hydrated Li+-, Na+-and K +-montmorillonite/polymer nanocomposites using large-scale molecular dynamics, Chem. Phys. Lett. 389 (4–6) (2004) 261–267.